

# Supplemental Data

## Excitation dynamics in a single core complex.

To characterize the excitation relaxation dynamics in a *Rba. sphaeroides* core complex, we considered the case in which the LH1 BChl farthest from the center ( $i = 14$ ) is excited first, corresponding to an initial condition of  $\rho(0) = |14\rangle\langle 14|$  for the evolution of  $\rho(t)$ . In this case, the initial state in Equations (9) and (10) corresponds to  $\mathbf{P}(0) = (1, 0)^T$  and  $\mathbf{P}(0) = (1, 0, 0, 0)^T$  for scheme I and scheme II, respectively.

Due to the large size of the systems ( $\sim 60$  BChls), we truncated the HEOM at the 2nd level, which corresponds to inclusion of 4th order system-bath coupling in a perturbative generalized master equation formalism (1). We included solely one temperature term in HEOM (see references (2; 3)), but employed the Markovian temperature correction term of Ishizaki and Tanimura (3) to account for the truncation of temperature terms in the bath correlation function.

Static disorder within the core complex, responsible for the inhomogeneous broadening of the absorption spectrum (4), was not included due to the computational expense of integrating the HEOM for ensembles of core complexes. The results presented still remain valid for comparative purposes between the different models of the core complex, since static disorder would be applied equally to each model. We also assume that each BChl is independently coupled to the environment. The inclusion of correlated environmental fluctuations between BChls is a non-trivial consideration and beyond the scope of the present study.

The evolution of the populations defined in Figure 4a for partition scheme I is presented in Figure S1 and Figure S2 for the models of LH1 with 52 BChls and PufX placed near the gaps of LH1 and in the center, respectively. The same is done for the same models for partition scheme II (Figure 4b) in Figure S3 and Figure S4. In these Figures are shown the time evolution of the respective populations as calculated by HEOM (green curves), a fit of the kinetic model to HEOM results (dashed red curves) and the results of the kinetic model with GF rate constants (dashed blue curves). Comparing the curves in Figures S1 and S2, one recognizes that for either placement of PufX, kinetic schemes fitting to HEOM density matrix evolution and kinetic schemes with GF transfer rate constants both agree closely with the HEOM population dynamics description.

From Figures S3 and S4 we discern that in the framework of partition scheme II, the kinetic model (dashed red curves) describes also well the population dynamics calculated by HEOM (green curves). The kinetic model with GF transfer rate constants (dashed blue curves) also provides a good match to the HEOM population dynamics for the side placement of PufX, but not for the placement of PufX near the gaps of LH1. This discrepancy between

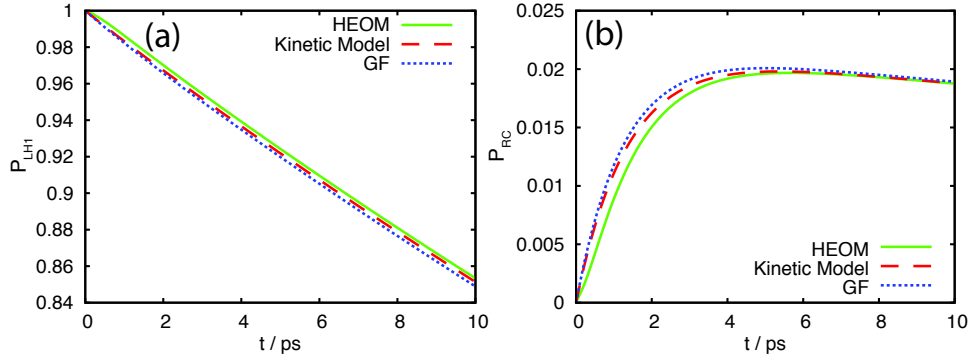


Figure S1: Evolution of the array populations for partition scheme I (Figure 4a) with 52 BChls in LH1 and PufX placed near the gaps of LH1 (Figure 3b). (a) Excited state population of BChls in LH1. (b) Excited state population of BChls in the RC.

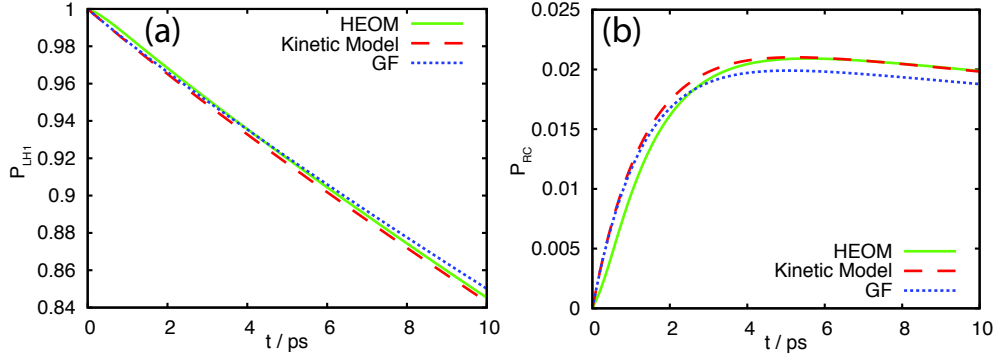


Figure S2: Evolution of the array populations for partition scheme I (Figure 4a) with 52 BChls in LH1 and center placement of PufX (Figure 3c). (a) Excited state population of BChls in LH1. (b) Excited state population of BChls in the RC.

the time evolution of the populations according to GF transfer rate constants (shown in Table 2) arises from the small intra-LH1 transfer rate constant of  $k_{LH1 \rightarrow LH1} = 1/82.5 \text{ ps}^{-1}$  (compared to  $1/35.3 \text{ ps}^{-1}$  obtained from the fit to  $\rho(t)$ ). This discrepancy is, however, not reflected in the calculations of light-harvesting efficiency and excitation lifetime presented in section 3.2. This is because  $k_{cs}$ ,  $k_{LH1 \rightarrow RC}$  and  $k_{RC \rightarrow LH1}$  are rate limiting for the light-harvesting efficiency and excitation lifetime, not  $k_{LH1 \rightarrow LH1}$ .

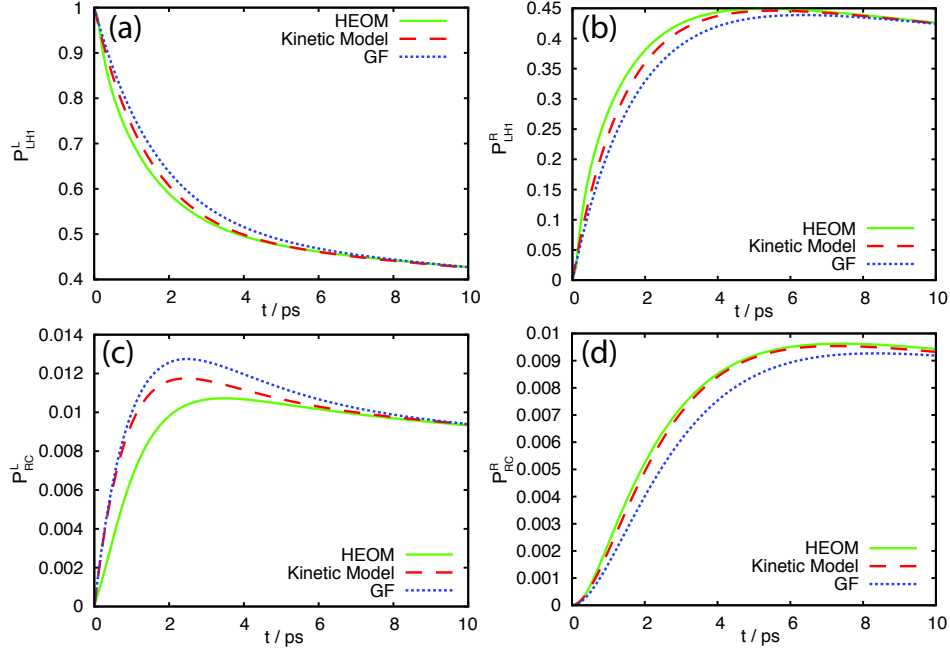


Figure S3: Evolution of the array populations for partition scheme II (Figure 4b) with 52 BChls in LH1 and PufX placed near the gaps of LH1 (Figure 3b). The initial excitation is located in the left half of LH1 in all calculations. (a) Excited state population of BChls in the left half of LH1. (b) Excited state population of BChls in the right half of LH1. (c) Excited state population of BChls in the left RC. (d) Excited state population of BChls in the right RC.

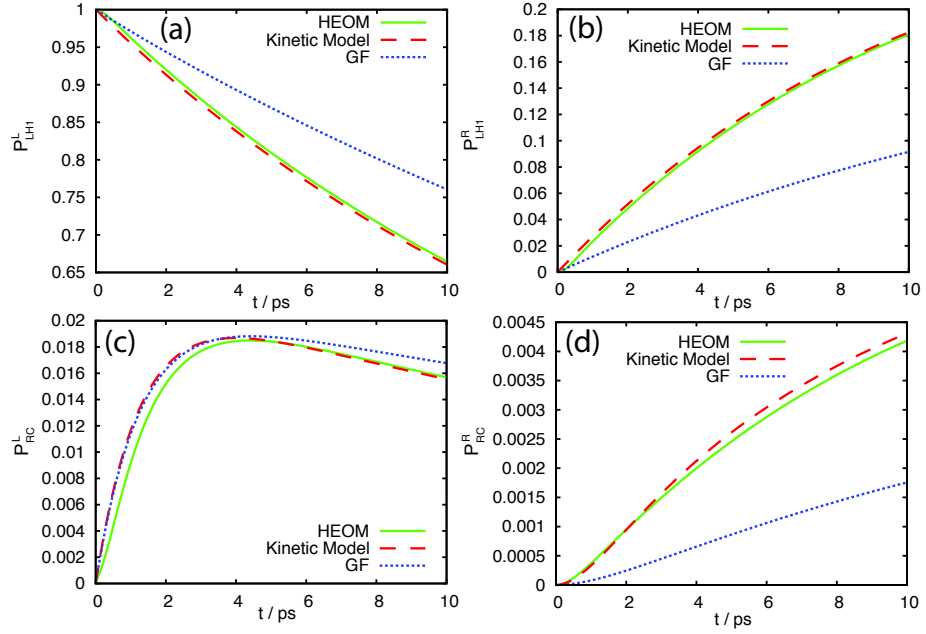


Figure S4: Evolution of the array populations for partition scheme II (Figure 4b) with 52 BChls in LH1 and center placement of PufX (Figure 3c). The initial excitation is located in the left half of LH1 in all calculations. (a) Excited state population of BChls in the left half of LH1. (b) Excited state population of BChls in the right half of LH1. (c) Excited state population of BChls in the left RC. (d) Excited state population of BChls in the right RC.

## References

1. Schröder, M., M. Schreiber, and U. Kleinekathöfer. 2007. Reduced dynamics of coupled harmonic and anharmonic oscillators using higher-order perturbation theory. *J. Chem. Phys.* 126:114102.
2. Strümpfer, J. and K. Schulten. 2009. Light harvesting complex II B850 excitation dynamics. *J. Chem. Phys.* 131:225101.
3. Ishizaki, A. and Y. Tanimura. 2005. Quantum dynamics of system strongly coupled to Low-Temperature colored noise bath: Reduced hierarchy equations approach. *J. Phys. Soc. Jpn.* 74:3131–3134.
4. Freiberg, A., M. Ratsep, K. Timpmann, and G. Trinkunas. 2009. Excitonic polarons in quasi-one-dimensional LH1 and LH2 bacteriochlorophyll a antenna aggregates from photosynthetic bacteria: A wavelength-dependent selective spectroscopy study. *Chem. Phys.* 357:102–112.